Meat and Muscle Biology™

# Differential Abundance of Mitochondrial Proteome Influences the Color Stability of Beef *Longissimus Lumborum* and *Psoas Major* Muscles

Ranjith Ramanathan[1], Mahesh N. Nair[2], Yifei Wang[3], Shuting Li[3], Carol M. Beach[4], Richard A. Mancini[5], Kaylin Belskie[5], and Surendranath P. Suman[3]*

[1]Department of Animal and Food Sciences, Oklahoma State University, Stillwater, OK 74078, USA
[2]Department of Animal Sciences, Colorado State University, Fort Collins, CO 80523, USA
[3]Department of Animal and Food Sciences, University of Kentucky, Lexington, KY 40546, USA
[4]Proteomics Core Facility, University of Kentucky, Lexington, KY 40506, USA
[5]Department of Animal Science, University of Connecticut, Storrs, CT 06269, USA
*Corresponding author. Email: spsuma2@uky.edu (Surendranath P. Suman)

**Abstract:** Mitochondrial functionality affects muscle-specific beef color stability. Nonetheless, the relationship between mitochondrial proteome and muscle-specific beef color stability is yet to be examined. Therefore, the objective of the present study was to differentiate the proteomes of mitochondria from beef *longissimus lumborum* (LL; color-stable muscle) and *psoas major* (PM; color-labile muscle) steaks during retail display. LL and PM muscles from 7 beef carcasses (USDA Choice; 48 h postmortem) were fabricated into 1.92-cm-thick steaks and were aerobically packaged and retail displayed for 6 d. Mitochondria were isolated on day 3 and 6, whereas instrumental color and biochemical attributes were evaluated on day 0, 3, and 6. Mitochondrial proteome was analyzed employing two-dimensional electrophoresis. The protein spots exhibiting 1.5-fold or more intensity differences ($P < 0.05$) between the muscles and display days were subjected to tryptic digestion and identified by tandem mass spectrometry. Whereas color stability decreased in both muscles during retail display, LL steaks demonstrated greater ($P < 0.05$) color stability during display than their PM counterparts. Mitochondria could not be isolated from PM steaks on day 6 because of extensive degradation. Seven proteins were differentially abundant ($P < 0.05$) in LL and PM on day 3 of display. In LL steaks, 7 proteins were more abundant ($P < 0.05$) on day 3 than on day 6 of retail display. The differentially abundant proteins were enzymes, binding proteins, and proteins involved in biosynthesis. These results indicated that differential abundance of mitochondrial proteome could also contribute to the variations in color stability of beef LL and PM muscles during retail display.

**Key words:** beef color, color stability, mitochondrial proteome, muscle specificity, proteomics
*Meat and Muscle Biology* 5(1): 16, 1–16 (2021) **doi:10.22175/mmb.11705**
Submitted 10 November 2020 Accepted 16 February 2021

## Introduction

Color of retail fresh meat is the most important quality affecting the purchase decisions of consumers (Faustman and Cassens, 1990; Mancini and Hunt, 2005; Suman et al., 2014; Neethling et al., 2017). In the United States, approximately 5% of fresh beef is wasted at retail stores owing to surface discoloration, leading to an estimated annual revenue loss of $3 billion (Maia Research Analysis, 2020). The interactions among myoglobin, mitochondria, metabolites, lipid oxidation, and sarcoplasmic proteome influence the color stability of fresh meats (Suman and Joseph, 2013; Abraham et al., 2017; Ramanathan et al., 2020a). Overall, the biochemical and cellular mechanisms promoting the formation of ferrous myoglobin forms (oxymyoglobin and deoxymyoglobin) can improve fresh beef color stability (Faustman et al., 2010). Myoglobin chemistry and mitochondrial

functionality in the muscle food matrix are closely interrelated (Ramanathan et al., 2019). Mitochondria remain functionally active in postmortem skeletal muscles and influence meat color either by providing reducing equivalents for metmyoglobin reduction (Belskie et al., 2015) or by competing with myoglobin for oxygen (Tang et al., 2005). Therefore, mitochondrial activity is critical to improving and maintaining the color stability of fresh beef (Ramanathan and Mancini, 2018; Ramanathan et al., 2020a, 2020b).

The US beef industry has been increasingly marketing individual muscles based on their quality attributes (Von Seggern et al., 2005). Beef muscles are categorized based on color stability traits (McKenna et al., 2005). More specifically, the beef *longissimus lumborum* (LL) is a color-stable muscle, whereas the *psoas major* (PM) is a color-labile muscle (Hunt and Hedrick, 1977; O'Keeffe and Hood, 1982; Ledward, 1985). Muscle-specific color stability in fresh beef has been examined employing high-throughput analytical tools in proteomics, and the differential abundance of sarcoplasmic proteome components (antioxidant proteins, chaperones, and glycolytic enzymes) has been attributed to variations in the color stability of beef LL and PM (Joseph et al., 2012; Nair et al., 2018a).

Mitochondrial content and biochemistry also are major contributing factors in beef color stability (Ramanathan et al., 2019). Beef PM has greater mitochondrial content than the LL counterparts (Mohan et al., 2010; Ke et al., 2017), primarily owing to differences in muscle fiber type (Hunt and Hedrick, 1977). Additionally, mitochondrial content in the PM decreased more rapidly than in the LL during retail display, indicating variations in mitochondrial degeneration rates (Ke et al., 2017). Mancini et al. (2018) examined mitochondrial functionality in beef LL and PM to explain muscle-dependent color stability and documented that oxygen consumption (OC) as well as metmyoglobin reducing activity (MRA) decreased more rapidly in mitochondria isolated from PM than those from LL.

Although the enzymes and proteins in the mitochondrial matrix are critical to biochemical pathways governing fresh meat color stability (Ramanathan and Mancini, 2018; Ramanathan et al., 2019, 2020a, 2020b), investigations have yet to be undertaken to characterize the relationship between mitochondrial proteome and muscle-specific beef color stability. Therefore, the objective of the present study was to differentiate the proteomes of mitochondria isolated from beef LL and PM steaks during retail display under aerobic conditions.

# Materials and Methods

## Beef muscle fabrication and retail display

The LL and PM muscles from the left sides of 7 ($n = 7$) beef carcasses (USDA Choice; A maturity) were obtained from a local packing plant within 48 h of harvest. Seven 1.92-cm-thick steaks were fabricated from the anterior halves of each muscle. From each muscle, 3 steaks were allotted for surface color evaluation (on 0, 3, and 6 d), the fourth steak was used for pH measurements, and the remaining 3 steaks were used to create myoglobin standards for myoglobin redox calculations. Following surface color measurements, steaks designated to 0, 3, and 6 d were cut in half perpendicular to the oxygen-exposed surface, but in random axis. These halves were assigned randomly for biochemical and proteome analyses; while one half was used for mitochondrial proteome profiling (on 3 and 6 d), the other half was used for OC and MRA measurements.

## Instrumental color

The surface color was measured on 0, 3, and 6 d. Steaks on 0-d display were placed on Styrofoam trays and overwrapped in polyvinylchloride film (15,500–16,275 $cm^3$ $O_2/m^2$/24 h at 23°C; E-Z Wrap Crystal Clear Polyvinyl Chloride Wrapping Film, Koch Supplies, Kansas City, MO) and bloomed at 4°C for 2 h before the color measurement. The packages were displayed in a coffin-type retail case at 4°C (1,612–2,152 lx; Philips Delux Warm White Fluorescent lamps, Andover, MA; color rendering index = 86; color temperature = 3,000 K) and were rotated every 24 h to minimize temperature variations within the case. The polyvinylchloride film was removed, and $L^*$ (lightness), $a^*$ (redness), and $b^*$ (yellowness) values (CIE, 1976) were recorded at 3 random locations on the light-exposed steak surfaces using a HunterLab MiniScan XE Plus (HunterLab Associates, Reston, VA) with 2.54-cm diameter aperture, illuminant A, and 10° observer angle (AMSA, 2012). The colorimeter was calibrated with standard black and white plates each day before the readings were taken. Additionally, the CIE (1976) $a^*$ and $b^*$ values were used to calculate hue angle and chroma (AMSA, 2012).

## Muscle pH

Samples from steaks assigned to 0 d of display from both LL and PM, visually devoid of fat and

connective tissue, were blended in an Omni tabletop mixer (Sorvall, Newton, CT). To determine pH, 10 g of pulverized steak that contained surface and interior was combined with 100 mL of deionized water and mixed for 30 s. The pH values were obtained by using an Accumet combination glass electrode connected to an Accumet 50 pH meter (Fisher Scientific, Fairlawn, NJ). Before measurements, the pH meter was standardized with pH 4 and 7 buffers.

### *Muscle oxygen consumption and metmyoglobin reducing activity*

The steak half assigned to MRA and OC was then bisected parallel to the oxygenated surface to expose the interior of the steak (resulting in 2 interior pieces). The first piece was used to measure MRA, and the second piece was used to measure muscle OC. The muscle OC was determined indirectly using the changes in oxymyoglobin level. A modified procedure of Madhavi and Carpenter (1993) was used to determine muscle OC on day 0, 3, and 6. Freshly cut steak interiors were allowed to oxygenate/bloom for 60 min at 4°C, vacuum packaged, and were scanned using a Hunter Lab MiniScan XE Plus spectrophotometer for reflectance from 400 nm to 700 nm to determine the initial percentage of oxymyoglobin (AMSA, 2012). OC (measured by conversion of oxymyoglobin to deoxymyoglobin) was induced by incubating samples at 30°C for 30 min. After incubation, the samples were rescanned immediately to determine remaining surface oxymyoglobin (AMSA, 2012). The reflectance (R) at 474, 525, 572, and 610 nm was converted to K/S values using $K/S = (1 - R)^2/2R$, in which K and S indicate absorption and scattering coefficient, respectively. These K/S values were then utilized in the following equations to calculate the percentage of oxymyoglobin and metmyoglobin (AMSA, 2012).

MRA was determined according to the protocol of Sammel et al. (2002). Samples ($1.5 \times 2.5 \times 2.5$ cm) were submerged in a 0.3% solution of sodium nitrite (Sigma, St. Louis, MO) for 20 min to facilitate metmyoglobin formation. The samples were then removed, blotted dry, vacuum packaged (Prime Source Vacuum Pouches, 4 mil, Koch Supplies Inc., Kansas City, MO), and scanned for reflectance spectra from 400 nm to 700 nm with a HunterLab MiniScan XE Plus spectrophotometer to determine pre-incubation metmyoglobin content (AMSA, 2012). The vacuum-packaged samples were incubated at 30°C for 2 h to induce metmyoglobin reduction. After incubation, the reflectance data were collected again to determine the post-incubation metmyoglobin content. The MRA was calculated using the following equation:

$$\begin{aligned}\text{MRA} = 100 \times [&(\%\text{ pre-incubation surface metmyoglobin} \\ &- \%\text{ post-incubation surface metmyoglobin}) \\ &\div \%\text{ pre-incubation surface metmyoglobin}]\end{aligned}$$

### *Statistical analysis of instrumental color and biochemical attributes data*

A split-plot experimental design was used to analyze the instrumental color, OC, and MRA data. The whole plot consisted of a randomized complete block design, in which carcass served as a block and muscles within a carcass were experimental units (LL or PM). In the subplot, steaks within a whole muscle served as experimental units assigned to day of display (0, 3, or 6). The random terms included carcass (Error A) and unspecified residual error (Error B). The data were analyzed using the Mixed procedure of SAS version 9.4 (SAS Institute Inc., Cary, NC), and the differences among means were detected using the least significant difference test at the 5% level.

$$\%\,\text{oxymyoglobin} = \frac{[\text{K/S610} \div \text{K/S525 for 100\% metmyoglobin} - \text{K/S610} \div \text{K/S525 for sample}]}{\left[\text{K/S610} \div \text{K/S525 for 100\% metmyoglobin} - \text{K/S610} \div \text{K/S525 for 100\% oxymyoglobin}\right]}$$

$$\%\,\text{metmyoglobin} = \frac{[\text{K/S572} \div \text{K/S525 for 100\% oxymyoglobin} - \text{K/S572} \div \text{K/S525 for sample}]}{[\text{K/S572} \div \text{K/S525 for 100\% oxymyoglobin} - \text{K/S572} \div \text{K/S525 for 100\% metmyoglobin}]}$$

To calculate muscle OC, the following equation was used:

$$\text{OC} = \%\text{pre-incubation surface oxymyoglobin} - \%\text{post-incubation surface oxymyoglobin}$$

### Isolation of mitochondria

Mitochondria were isolated from the beef muscles according to Lanari and Cassens (1991). On 3 and 6 d of display, LL or PM muscle tissue (35 g) was minced finely and suspended in 70 mL of mitochondrial suspension buffer (125 mM sucrose, 5 mM 4-(2-hydroxyethyl)-1-piperazineethanesulfonic acid). The suspension was hydrolyzed for 15 min with proteinase K (protease/tissue, 1.0 mg/g for LL or 0.5 mg/g for PM), and the pH was maintained between 7.0 and 7.2. The suspension was diluted with mitochondrial isolation buffer (125 mM sucrose, 125 mM Tris-HCl, 10 mM KCl, 25 mM ethylenediaminetetraacetic acid, and 0.2% bovine serum albumin [pH 7.2]) to 350 mL and homogenized using a Kontes Duall grinder (Vineland, NJ), passed through a Wheaton Potter-Elvehjem grinder (Millville, NJ), and centrifuged for 20 min at 900 × *g* in a Sorvall refrigerated RC-5B centrifuge (Thermo Fisher Scientific, Waltham, MA). The resulting supernatant was passed through double-layered cheesecloth and centrifuged for 15 min at 14,000 × *g*. The pellet was washed twice and suspended in mitochondrial suspension buffer at pH 7.2. All steps were performed at 0°C to 4°C. Mitochondrial protein content was determined using a bicinchoninic acid protein assay, and the total mitochondrial yield was reported as milligrams per gram of tissue (Grubbs et al., 2013; Ke et al., 2017).

### Mitochondrial proteome solubilization

The aliquots of suspended mitochondria were centrifuged to pellet the mitochondria. The supernatant was discarded, and the crude mitochondrial pellet with 200 µL of the extraction buffer (8.3 M urea, 2 M thiourea, 2% 3-[(3-cholamidopropyl) dimethylammonio]-1-propanesulfonate, and 1% dithiothreitol [DTT] [pH 8.5]) was shaken vigorously for 30 min at room temperature. Samples were centrifuged at 10,000 × *g* for 30 min. The supernatant was filtered, and the protein concentration was determined using a 2D Quant assay (GE Healthcare Life Sciences, Piscataway, NJ).

### Two-dimensional electrophoresis

The mitochondrial proteome (900 µg) was mixed with DeStreak Rehydration Solution (GE Healthcare Life Sciences, Piscataway, NJ) with 2 mM DTT and 0.5% immobilized pH gradient (IPG) buffer (pH 3–10; GE Healthcare Life Sciences, Piscataway, NJ) to a total volume of 300 µL. The mix was loaded onto IPG strips (pH 3–10; 17 cm) and was subjected to passive rehydration for 16 h. First-dimension isoelectric focusing of the IPG strips was done in a Protean IEF cell system (Bio-Rad, Hercules, CA) by applying a linear increase in voltage initially and a final rapid voltage ramping to attain a total of 80 kVh. Subsequently, the IPG strips were equilibrated with equilibration buffer I (6 M urea, 0.375 M Tris-HCl [pH 8.8], 2% sodium dodecyl sulfate [SDS], 20% glycerol, 2% w/v DTT; Bio-Rad) followed by equilibration buffer II (6 M urea, 0.375 M Tris-HCl [pH 8.8], 2% SDS, 20% glycerol, 2.5% w/v iodoacetamide; Bio-Rad) for 15 min each. Second-dimension separation of proteins was done by 13.5% SDS polyacrylamide gel electrophoresis (38.5:1 ratio of acrylamide to bis-acrylamide; SDS-polyacrylamide gel electrophoresis) using a Protean XL system (Bio-Rad, Hercules, CA). The gels were stained with colloidal Coomassie Blue for 48 h and destained in deionized distilled water for 48 h or until sufficient background was cleared.

### Gel image analysis

The digital images of the destained gels were captured using Versa Doc imager (Bio-Rad, Hercules, CA) and were analyzed using PDQuest software (Bio-Rad, Hercules, CA). Images were first subjected to automatic spot detection and matching optimized by the aid of landmark protein spots. The relative volume of each spot was normalized as a percentage of the total volume of all the spots detected on the gel (Joseph et al., 2012). For each spot in a given sample, spot quantity values in duplicate gels were averaged for statistical analysis (Nair et al., 2018a; Zhai et al., 2018). A spot was considered to be differentially abundant when it demonstrated 1.5-fold intensity difference between the treatments associated with $P < 0.05$ in a pairwise Student *t* test.

### Protein identification by tandem mass spectrometry

Protein spots differentially abundant between the treatments were excised from the gel using pipet tips. The spots were destained by two 30-min washes with 50 mM $NH_4HCO_3$/50% $CH_3CN$ followed by vortexing for 10 min and drying using a vacuum centrifuge. Proteins in the gel were reduced by the addition of 50 mM $NH_4HCO_3$ containing 10 mM DTT and incubation at 57°C for 30 min. Further, the proteins were alkylated by the addition of 50 mM $NH_4HCO_3$ containing 50 mM iodoacetamide and incubation for 30 min in the dark at room temperature. The gel pieces were washed twice with 50 mM $NH_4HCO_3$ and once with $CH_3CN$ and partially dried in a vacuum centrifuge. Dried gel pieces were rehydrated for 1 h (on ice) with

a solution of 40 mM $NH_4HCO_3$/9% $CH_3CN$, containing proteomic grade trypsin (Sigma, St. Louis, MO) at a concentration of 20 ng/μL. An additional volume of 40 mM $NH_4HCO_3$/9% $CH_3CN$ was added to cover the sample, and the gel was incubated for 18 h at 37°C. Peptide extraction from the gel was done by sonication in 0.1% trifluoroacetic acid for 10 min followed by vortexing for 10 min. Extraction was repeated with 50% $CH_3CN$/0.1% trifluoroacetic acid. The extracts were combined, and the volume was decreased to eliminate most of the acetonitrile. The peptide extracts were desalted and concentrated by solid phase extraction using a 0.1–10 μL pipet tip (Sarstedt, Newton, NC) packed with 1 mm of Empore C-18 (3M, St. Paul, MN), and peptides were eluted in 5 μL of 50% $CH_3CN$/0.1% trifluoroacetic acid. Desalted peptide extracts (0.3 μL) were spotted onto an Opti-TOF 384 well insert (Applied Biosystems, Foster City, CA) with 0.3 μL of 5 mg/mL α-cyano-4-hydroxycinnamic acid (Aldrich, St. Louis, MO) in 50% $CH_3CN$/50% 0.1% trifluoroacetic acid. Crystallized samples were washed with cold 0.1% trifluoroacetic acid and were analyzed using a 4800 MALDI TOF-TOF Proteomics Analyzer (Applied Biosystems). The initial matrix-assisted laser desorption ionization mass spectrometry (MS) spectrum was acquired for each spot with 400 laser shots per spectrum. From that, a maximum of 15 peaks with a signal-to-noise ratio of >20 were automatically selected for tandem mass spectrometry (MS-MS) analysis (1,000 shots per spectrum) by post-source decay. Peak lists from the MS-MS spectra were submitted for database similarity search using Protein Pilot version 2.0 (Applied Biosystems), and the search was performed in the Swiss Prot and National Center for Biotechnology Information database to identify the proteins using search parameters (search type: identification; enzyme: trypsin; database: bovine NCBInr; search effort: thorough; unused cutoff > 1.30, 95% confidence).

The differentially abundant proteins were matched against the STRING database (Szklarczyk et al., 2015) to determine the protein–protein interaction networks (on the influence of muscle source and retail display), in which the network nodes represented the proteins and the lines indicated functional associations.

## Results and Discussion

### *Instrumental color and biochemical traits*

The PM steaks had greater pH than LL steaks on day 0 of display (LL = 5.56, PM = 5.63; $P < 0.05$; standard error of the mean = 0.02). There was a muscle × display day interaction ($P < 0.05$) for instrumental color parameters (Table 1). The LL steaks had greater ($P < 0.05$) $L^*$, $a^*$, $b^*$, and chroma values than the PM counterparts throughout display. Although the $a^*$, $b^*$, and chroma values decreased ($P < 0.05$) between 0 and 6 d of retail display in both muscles, the decline was less for LL steaks compared with PM ones. The $L^*$ value increased ($P < 0.05$) for both muscles from day 0 to day 3 and then decreased on day 6. On day 3 and 6, PM steaks exhibited greater ($P < 0.05$) hue angle than LL steaks. Whereas hue increased ($P < 0.05$) in PM steaks during display, it did not change ($P > 0.05$) in LL steaks.

Muscle source and display day influenced ($P < 0.05$; Table 2) MRA and OC. The LL steaks demonstrated greater ($P < 0.05$) MRA and lower ($P < 0.05$) OC than their PM counterparts during display. Both MRA and OC decreased ($P < 0.05$) in LL and PM steaks between day 0 and day 6. While MRA remained stable ($P > 0.05$) until day 3, it declined ($P < 0.05$) in both muscles between day 3 and day 6. On the other hand, OC decreased ($P < 0.05$) on day 3 and remained stable ($P > 0.05$) until day 6 in both LL and PM steaks.

The results of instrumental color (Table 1) and biochemical attributes (Table 2) reiterated that the LL is a color-stable beef muscle, whereas the PM is a color-labile muscle. These findings are in agreement with several previous studies (Hunt and Hedrick, 1977; O'Keeffe and Hood, 1982; Madhavi and Carpenter, 1993; McKenna et al., 2005; Seyfert et al., 2006; Kim et al., 2009; Mancini et al., 2009; Joseph et al., 2012;

**Table 1.** Instrumental color of beef LL and PM steaks ($n = 7$) during refrigerated retail display (4°C) under aerobic packaging

| | | Days of retail display | | | |
|---|---|---|---|---|---|
| Parameter | Muscle | 0 | 3 | 6 | SEM |
| $L^*$ value | LL | 40.98$^{b}$ | 43.08$^{a}$ | 38.89$^{c}$ | 0.80 |
| | PM | 36.19$^{d}$ | 40.13$^{bc}$ | 33.21$^{e}$ | |
| $a^*$ value | LL | 31.87$^{a}$ | 29.60$^{b}$ | 28.62$^{b}$ | 0.55 |
| | PM | 29.49$^{b}$ | 19.73$^{c}$ | 16.85$^{d}$ | |
| $b^*$ value | LL | 24.91$^{a}$ | 23.03$^{b}$ | 22.72$^{b}$ | 0.53 |
| | PM | 23.08$^{b}$ | 20.38$^{c}$ | 16.68$^{d}$ | |
| Hue angle | LL | 38.02$^{b}$ | 37.79$^{b}$ | 38.40$^{b}$ | 0.94 |
| | PM | 38.07$^{b}$ | 46.23$^{a}$ | 44.82$^{a}$ | |
| Chroma | LL | 40.45$^{a}$ | 37.53$^{b}$ | 36.60$^{b}$ | 0.56 |
| | PM | 37.45$^{b}$ | 28.53$^{c}$ | 23.78$^{d}$ | |

[a–e]Means without common superscripts within a parameter are different ($P < 0.05$).

LL = *longissimus lumborum*; PM = *psoas major*; SEM = standard error of the mean.

**Table 2.** MRA and OC of beef LL and PM steaks ($n = 7$) during refrigerated retail display (4°C) under aerobic packaging

| | | Days of retail display | | | |
|---|---|---|---|---|---|
| Parameter | Muscle | 0 | 3 | 6 | SEM |
| MRA | LL | 66.87$^{ax}$ | 64.30$^{ax}$ | 60.97$^{bx}$ | 1.76 |
| | PM | 52.17$^{ay}$ | 50.52$^{ay}$ | 40.80$^{by}$ | |
| OC | LL | 32.53$^{ay}$ | 15.43$^{by}$ | 10.93$^{by}$ | 2.13 |
| | PM | 47.57$^{ax}$ | 24.29$^{bx}$ | 20.75$^{bx}$ | |

$^{a–b}$Means without common superscripts in a row are different ($P < 0.05$).

$^{x–y}$Means without common superscripts in a column within a parameter are different ($P < 0.05$).

LL = *longissimus lumborum*; MRA = metmyoglobin reducing activity; OC = oxygen consumption; PM = *psoas major*; SEM = standard error of the mean.

Canto et al., 2016; Nair et al., 2018a), which reported greater color stability in beef LL than in PM.

## *Mitochondrial proteome profile*

Mitochondria could not be isolated from PM steaks on day 6 because of extensive degradation. Previous research also reported negligible PM mitochondrial yield with storage time (Mancini et al., 2018). Therefore, proteome analyses were accomplished only on mitochondria isolated from LL steaks on day 3 and day 6 as well as PM steaks on day 3. This allowed for evaluating the effect of muscle (LL vs. PM on day 3) and retail display (LL on day 3 vs. LL on day 6) on mitochondrial proteome profile.

## *Muscle source influences mitochondrial proteome profile*

Image analyses of gels identified 7 proteins differentially abundant in the mitochondrial proteome isolated from beef LL and PM steaks after 3-d refrigerated retail display (Figure 1). The identified proteins are listed in Table 3 along with accession number, ProtScore, and sequence coverage. While 2 proteins were more abundant in day-3 LL steaks, 5 were overabundant in PM steaks. The differentially abundant proteins were enzymes, binding proteins, and proteins involved in biosynthesis. The network of interacting proteins generated using the STRING database (Figure 2) identified 7 proteins as key nodes in biological interactions on the influence of muscle source. These results indicated the contribution of mitochondrial proteome in muscle-specific beef color stability.

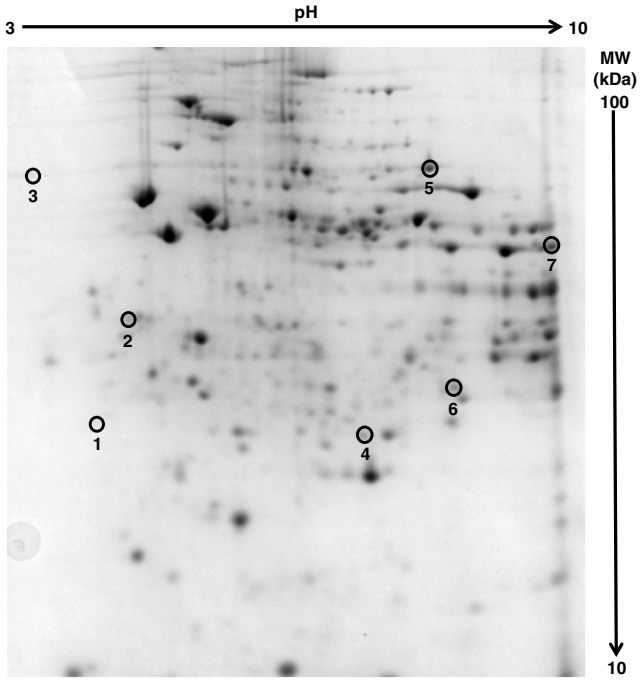


**Figure 1.** Representative two-dimensional gel electrophoresis map of mitochondrial proteome extracted from beef *psoas major* steak. Seven protein spots differentially abundant in *psoas major* and *longissimus lumborum* mitochondria are circled and numbered. MW = molecular weight.

**Succinyl-coenzyme A ligase subunit beta, mitochondrial.** Succinyl-coenzyme A ligase subunit beta (SUCLA2), located in the mitochondrial matrix, is responsible for catalyzing the reversible conversion of succinyl coenzyme A (CoA) and adenosine diphosphate (ADP) to succinate and adenosine triphosphate (ATP), which represents the only step of substrate-level phosphorylation in the tricarboxylic acid (TCA) cycle (Johnson et al., 1998; Ostergaard, 2008). The beta subunit binds the substrate succinate, whereas the binding sites for CoA and phosphate are located in the alpha subunit. SUCLA2 was more abundant in PM mitochondria than in LL mitochondria. The greater content of SUCLA2 involved in aerobic ATP synthesis possibly indicates a greater OCR in PM steaks than in LL steaks. Beef PM is an oxidative muscle with more red fibers and more mitochondrial content than LL, which is a glycolytic muscle (Hunt and Hedrick, 1977; Kirchofer et al., 2002; Mancini et al., 2018; Ramanathan and Mancini, 2018). A greater mitochondrial content in PM than in LL could lead to a greater OCR (Table 2) and result in lower oxygen partial pressure inside the meat. A lower oxygen partial pressure in the range of 1% to 3% can promote metmyoglobin formation. A lower MRA coupled with lower oxygen partial pressure can increase PM discoloration (Ramanathan et al., 2019).

**Ubiquinone biosynthesis protein coenzyme Q9, mitochondrial.** Ubiquinone biosynthesis protein

**Table 3.** Identity and functional roles of differentially abundant proteins in mitochondrial proteome of beef PM and LL steaks after 3-d refrigerated retail display

| Spot[a] | Protein | Accession number | ProtScore | Sequence coverage (%) | Overabundant treatment | Spot ratio | Function |
|---|---|---|---|---|---|---|---|
| 1 | Succinyl-CoA ligase subunit beta, mitochondrial | Q148D5 | 8.01 | 10.4 | PM | 2.27[b] | ATP synthesis |
| 2 | Ubiquinone biosynthesis protein COQ9 | Q2NL34 | 4.00 | 17.6 | PM | 4.00[b] | Biosynthesis of ubiquinone |
| 3 | ATP synthase subunit beta, mitochondrial | P00829 | 12.00 | 18.2 | PM | 1.72[b] | ATP synthesis |
| 4 | ES1 protein homolog, mitochondrial | Q3T0U3 | 6.07 | 36.5 | PM | 1.70[b] | Protection of mitochondrial functionality |
| 5 | Very long-chain specific acyl-CoA dehydrogenase | P48818 | 12.00 | 13.1 | PM | 14.29[b] | Fatty acid beta-oxidation |
| 6 | Carbonic anhydrase 3 | Q3SZX4 | 15.37 | 44.2 | LL | 1.66[c] | Hydration of carbon dioxide |
| 7 | Aspartate aminotransferase, mitochondrial | P12344 | 12.98 | 24.4 | LL | 1.78[c] | Amino acid metabolism |

[a]Spot number refers to the numbered spots in gel image (Figure 1). Spots are identified by accession number (UniProt), ProtScore, and sequence coverage of peptides.

[b]Spot ratio of PM/LL.

[c]Spot ratio of LL/PM.

ATP = adenosine triphosphate; CoA = coenzyme A; COQ9 = coenzyme Q9; LL = *longissimus lumborum*; PM = *psoas major*.

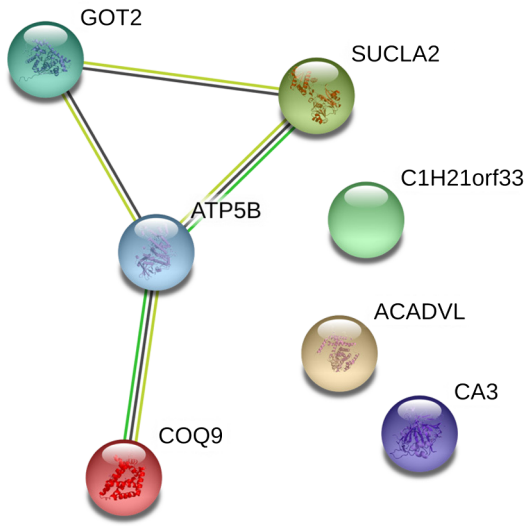


**Figure 2.** Protein–protein interaction network of differentially abundant proteins in the mitochondrial proteome of beef *psoas major* and *longissimus lumborum* steaks after 3-d refrigerated retail display. The interacting proteins were identified using STRING 11.0 software (Szklarczyk et al., 2015). The nodes represent proteins from a *Bos taurus* database, whereas the lines (light green = text mining evidence; black = co-expression evidence; green = gene neighborhood evidence) indicate predicted functional annotations. ACADVL = very long-chain specific acyl-CoA dehydrogenase; ATP5B = ATP synthase subunit beta; C1H21orf33 = ES1 protein homolog; CA3 = carbonic anhydrase 3; COQ9 = ubiquinone biosynthesis protein COQ9; GOT2 = aspartate aminotransferase; SUCLA2 = succinyl-CoA ligase subunit beta.

coenzyme Q9 (COQ9) enables synthesis of ubiquinone through its lipid-binding capacity (Lohman et al., 2014) and was more abundant in the PM than in the LL. Ubiquinone, also known as coenzyme Q, is a critical component of mitochondrial electron transport chain and is responsible for shuttling electrons from complex I and II to complex III in inner mitochondrial membrane (Lohman et al., 2014). Moreover, ubiquinone plays an important role in mitochondrial energy production and is a prominent source of reactive oxygen species (Wang and Hekimi, 2016). The greater abundance of ubiquinone biosynthesis protein COQ9 in PM mitochondria than in LL mitochondria could be a reflection of the differences in generating reactive oxygen species, which accelerate lipid oxidation (Faustman et al., 2010) and subsequent rapid discoloration in the PM (Ramanathan et al., 2020a, 2020b).

**ATP synthase subunit beta, mitochondrial.** ATP synthase subunit beta (ATP5F1B) is a catalytic subunit of ATP synthase, catalyzing the rate-limiting step of ATP synthesis in eukaryotic cells (Izquierdo, 2006). A greater abundance of ATP5F1B was observed in PM mitochondria compared with LL mitochondria. ATP synthase is involved in oxidative energy metabolism in mitochondria and is responsible for synthesizing ATP from ADP, utilizing an electrochemical gradient of protons through the inner membrane during oxidative phosphorylation (Xu et al., 2013). The differential abundance of this oxidative enzyme could be attributed to the variations in muscle fiber types; PM is an oxidative muscle, whereas LL is a glycolytic muscle (Hunt and Hedrick, 1977; Kirchofer et al.,

2002). Shen et al. (2015) examined glycolysis-related gene expression in the muscle tissue of Tibetan pigs and documented a greater expression of the ATP synthase genes in slow-oxidative type muscles than in fast-glycolytic type muscles from pigs. Similarly, Yu et al. (2017b) also observed a greater abundance of ATP5F1B in the PM of Holstein cattle compared with the LL. In contrast, ATP5F1B was positively correlated with redness and MRA in LL muscles from Chinese Luxi yellow cattle (Wu et al., 2016).

**ES1 protein homolog, mitochondrial.** The ES1 protein homolog is involved in mitochondrial biogenesis in diverse cell types, including skeletal muscle cells (Gueugneau et al., 2014; Masuda et al., 2016). In the present study, ES1 protein homolog was overabundant in PM steaks compared with LL steaks. Recently, Utsumi et al. (2020) documented that ES1 protein homolog was localized in the mitochondrial intermembrane space of porcine retinal cells and contributed to the protection of mitochondrial functionality. Gueugneau et al. (2014) observed lower abundance of ES1 protein homolog in muscles in older humans compared with muscles in younger ones, indicating its potential role in ageing. Furthermore, ES1 was found to promote enlargement of individual mitochondria in the cone cells of zebrafish retinas, and the enlarged mitochondria were capable of producing increased energy (Masuda et al., 2016). Although ES1 homolog has been reported in several clinical studies, its role in meat color remains largely unknown. Beef PM is an oxidative muscle demonstrating greater OCR than LL (O'Keeffe and Hood, 1982; Ramanathan et al., 2018). The overabundance of ES1 protein homolog may have led to enlargement of mitochondria and could have contributed to the greater OC (Table 2) and lower color stability (Table 1) observed in PM compared with LL.

**Very-long-chain acyl-CoA dehydrogenase.** Very-long-chain acyl-CoA dehydrogenase (VLCAD) is one of the 5 acyl-CoA dehydrogenases responsible for catalyzing the initial rate-limiting step of mitochondrial fatty acid beta-oxidation (McAndrew et al., 2008). VLCAD was more abundant in PM mitochondria than in LL mitochondria. In agreement, Yu et al. (2017b) observed greater levels of VLCAD in the PM than in the LL of Holstein cattle. The acyl-CoA fatty acids undergo chain-length–specific dehydrogenation by acyl-CoA dehydrogenases. VLCAD binds to the mitochondrial inner membrane and has a high specificity to C12 to C24 acyl-CoA fatty acids (Henriques et al., 2010). Beta-oxidation of fatty acids increases the generation of reactive oxygen species (St-Pierre et al., 2002; Schlater et al., 2014), which in turn can accelerate myoglobin oxidation compromising color stability (Faustman et al., 2010; Suman and Joseph, 2013). Previous research also noted greater lipid oxidation in PM than LL (Joseph et al., 2012; Canto et al., 2016; Ke et al., 2017). The overabundance of VLCAD in the PM indicated a greater level of beta-oxidation and lipid oxidation–induced surface discoloration compared with the LL.

**Carbonic anhydrase 3.** Carbonic anhydrase 3 (CA3) is a metalloenzyme responsible for proton homeostasis, through catalyzing the interconversion of carbon dioxide and water to carbonic acid and protons (Silverman and Lindskog, 1988; Lindskog, 1997; Christianson and Fierke, 1996). In the present study, CA3 was overabundant in the mitochondria from LL steaks compared with PM steaks. CA3 was suggested as a potential indicator of increased glycolysis in skeletal muscles (Vasilaki et al., 2007; Schilling et al., 2017). The greater abundance of CA3 observed in the LL compared with the PM indicated the predominance of glycolytic metabolism previously reported in the LL muscle (O'Keeffe and Hood, 1982; Hamelin et al., 2007). Furthermore, glycolytic metabolism promotes meat color stability by facilitating the production of NADH in postmortem muscle (Ramanathan et al., 2020a, 2020b), which is an important cofactor in enzymatic and nonenzymatic metmyoglobin reduction (Ramanathan and Mancini, 2010; Ramanathan et al., 2018). Therefore, logically muscles with a greater abundance of CA3 would be more color stable, which could explain the greater color stability of the LL.

**Aspartate aminotransferase, mitochondrial.** Aspartate aminotransferase (GOT2) was more abundant in LL mitochondria than in PM mitochondria. GOT2 plays a key role in amino acid metabolism through its involvement in transamination reaction; it catalyzes the transfer of amino group from aspartate to ketoglutarate leading to the formation of oxaloacetate and glutamate. Oxaloacetate is necessary for the TCA cycle, which regenerates the postmortem pool of NADH via the electron transport chain, ultimately reducing metmyoglobin localized near the mitochondrial outer membrane (Mohan et al., 2010). The greater concentration of GOT2 in the LL could lead to higher oxaloacetate production, and therefore greater MRA (Table 2) and better color stability (Table 1). Interestingly, GOT2 has been proposed as a potential biomarker

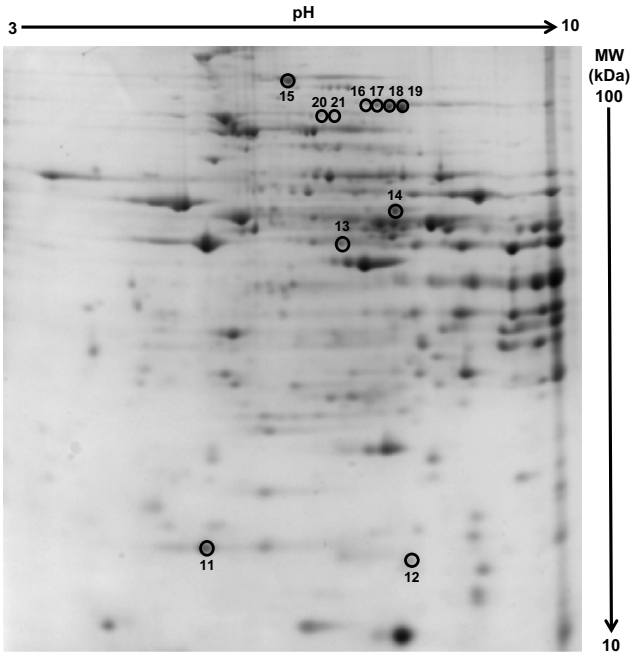


**Figure 3.** Representative two-dimensional gel electrophoresis map of mitochondrial proteome extracted from beef *longissimus lumborum*. Eleven protein spots differentially abundant in mitochondria isolated after 3 and 6 d of refrigerated retail display are circled and numbered. MW = molecular weight.

for dark-cutting beef; Wu et al. (2020) documented the overabundance of GOT2 in the mitochondrial proteome from dark-cutting beef LL.

### *Retail display influences mitochondrial proteome profile of beef LL steaks*

Gel image analyses indicated that 11 protein spots were differentially abundant between the LL steaks from day 3 and day 6 (Figure 3). MS-MS identified 7 proteins from the 11 spots because 2 proteins were present in multiple spots. These 7 proteins were more abundant in the mitochondria isolated from beef LL steaks on day 3 of refrigerated display (LL3) compared with those from LL steaks on day 6 (LL6), indicating that the duration of display impacted mitochondrial functionality and biochemistry. The differentially abundant proteins were enzymes and binding proteins (Table 4). In the protein–protein network generated using the STRING database, 7 proteins appeared as key nodes in biological interactions on the impact of retail display in LL steaks (Figure 4).

**Sarcoplasmic/endoplasmic reticulum $Ca^{2+}$-ATPase, chain A.** The sarcoplasmic/endoplasmic reticulum $Ca^{2+}$-ATPase (SERCA) is an integral membrane protein in skeletal muscles (Møller et al., 2010), where it is involved in calcium homeostasis (Chai et al., 2010; Nierobisz, 2010). SERCA was more abundant in LL3 steaks compared with LL6 ones. The presence of SERCA in the mitochondrial proteome could be attributed to the sarcoplasmic/endoplasmic reticulum

**Table 4.** Identity and functional roles of differentially abundant proteins in mitochondrial proteome of beef LL3 and LL6

| Spot[a] | Protein | Accession number | ProtScore | Sequence coverage (%) | Overabundant treatment | Spot ratio[b] | Function |
|---|---|---|---|---|---|---|---|
| 11 | Sarcoplasmic/endoplasmic reticulum $Ca^{2+}$-ATPase, chain A | Q0VCY0 | 10.36 | 5.5 | LL3 | 2.43 | Calcium homeostasis |
| 12 | Creatine kinase M-type | Q9XSC6 | 8.99 | 12.6 | LL3 | 2.56 | Energy metabolism |
| 13 | Pyruvate dehydrogenase E1 component subunit alpha, somatic form, mitochondrial | A7MB35 | 21.18 | 25.1 | LL3 | 1.62 | Decarboxylation of pyruvate |
| 14 | NADH dehydrogenase (ubiquinone) flavoprotein 1, mitochondrial | P25708 | 19.15 | 34.9 | LL3 | 1.90 | Electron transport chain |
| 15 | 2-oxoglutarate dehydrogenase, mitochondrial | Q148N0 | 21.82 | 11.5 | LL3 | 1.85 | Decarboxylation of alpha-ketoglutarate in citric acid cycle |
| 16 | Mitochondrial aconitase 2 | P20004 | 16.01 | 15.4 | LL3 | 1.81 | Isomerization of citrate to isocitrate |
| 17 | Mitochondrial aconitase 2 | P20004 | 20.97 | 21.9 | LL3 | 2.22 | Isomerization of citrate to isocitrate |
| 18 | Mitochondrial aconitase 2 | P20004 | 20.77 | 20.4 | LL3 | 2.59 | Isomerization of citrate to isocitrate |
| 19 | Mitochondrial aconitase 2 | P20004 | 24.60 | 23.7 | LL3 | 3.69 | Isomerization of citrate to isocitrate |
| 20 | Transferrin | Q29443 | 10.02 | 9.2 | LL3 | 2.17 | Iron binding |
| 21 | Transferrin | Q29443 | 10.36 | 7.8 | LL3 | 1.66 | Iron binding |

[a]Spot number refers to the numbered spots in the gel image (Figure 3). Spots are identified by accession number (UniProt), ProtScore, and sequence coverage of peptides.

[b]Spot ratio of LL3/LL6.

LL3 = beef *longissimus lumborum* steaks on 3 d of refrigerated retail display; LL6 = beef *longissimus lumborum* steaks on 6 d of refrigerated retail display.

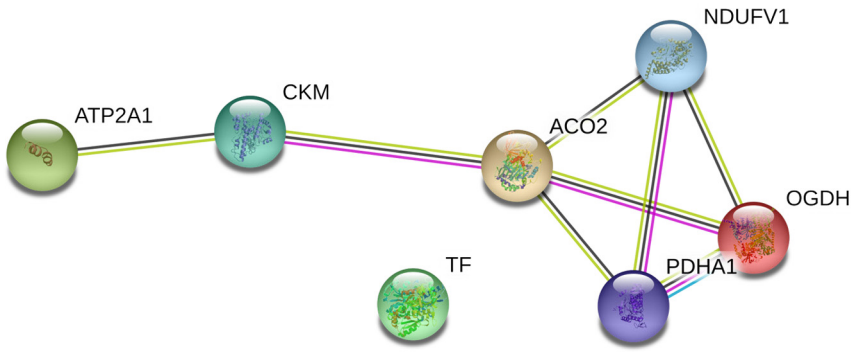


**Figure 4.** Protein–protein interaction network of differentially abundant proteins in the mitochondrial proteome of beef *longissimus lumborum* steaks after 3 and 6 d of refrigerated retail display. The interacting proteins were identified using STRING 11.0 software (Szklarczyk et al., 2015). The nodes represent proteins from a *Bos taurus* database, whereas the lines (light green = text mining evidence; black = co-expression evidence; pink = experimentally determined evidence; blue = evidence from curated databases) indicate predicted functional annotations. ACO2 = mitochondrial aconitase 2; ATP2A1 = sarcoplasmic/endoplasmic reticulum $Ca^{2+}$-ATPase, chain A; CKM = creatine kinase M-type; NDUFV1 = NADH dehydrogenase (ubiquinone) flavoprotein 1; OGDH = 2-oxoglutarate dehydrogenase; PDHA1 = pyruvate dehydrogenase E1 component subunit alpha, somatic form; TF = transferrin.

(SR/ER)-mitochondrial physical linkages, also known as SR/ER-mitochondria tethers (Csordas et al., 2006; Eisner et al., 2013). These physical linkages between SR/ER and mitochondria in skeletal (Rossi et al., 2009) and cardiac (Csordas et al., 2010) muscles influence $Ca^{2+}$ dynamics at the SR/ER-mitochondrial interface and allow direct coupling between $Ca^{2+}$ release from the SR/ER and mitochondrial $Ca^{2+}$ uptake (Szabadkai et al., 2006). Mitochondrial $Ca^{2+}$ uptake has been reported to regulate aerobic metabolism (Hajnoczky et al., 1995) and mitochondrial motility (Yi et al., 2004). In muscle cells, the $Ca^{2+}$ ions stored in the sarcoplasmic reticulum are released into cytosol for muscle contraction (Toyoshima and Inesi, 2004). At the end of the contraction cycle, SERCA is responsible for pumping 2 $Ca^{2+}$ ions back to the lumen of sarcoplasmic reticulum at the expense of the hydrolysis of 1 ATP molecule, in order to restore the resting $Ca^{2+}$ concentration (Fleischer and Inui, 1989; Bianchini et al., 2014). Although the role of SERCA has been reported in pale, soft, exudative pork (Guo et al., 2016), how this protein influences fresh meat color is not clearly understood. Zhang et al. (2011) reported that oxidative stress could lead to decreased SERCA activity, and the greater abundance of SERCA in LL3 compared with LL6 could be possibly due to the increase in oxidative stress during retail display.

**Creatine kinase M-type.** Creatine kinase M-type, a key enzyme in energy metabolism, is responsible for catalyzing the reversible reaction of phosphocreatine and ADP, generating creatine and ATP (Wallimann et al., 1992; McLeish and Kenyon, 2005). Previous studies reported that creatine exhibited antioxidant properties through its free radical scavenging ability (Lawler et al., 2002; Sestili et al., 2006). Creatine kinase M-type was more abundant in the mitochondria from LL3 than LL6. The greater content of creatine kinase M-type in mitochondria from LL3 steaks indicates a greater level of creatine compared with LL6 steaks, which could have contributed to a better color stability in LL3 steaks. The antioxidant properties of creatine could minimize myoglobin oxidation and improve color stability in beef LL muscle (Lawler et al., 2002; Sestili et al., 2011; Canto et al., 2015). In agreement, a positive correlation between creatine kinase M-type and beef color stability has been reported previously (Joseph et al., 2012; Marino et al., 2014; Canto et al., 2015; Nair et al., 2016, 2018a, 2018b). Creatine kinase M-type is considered a positive biomarker in color-stable beef muscles (Gagaoua et al., 2020) and correlated positively with surface redness in beef LL (Joseph et al., 2012; Nair et al., 2018a; Yang et al., 2018) and *semimembranosus* (Nair et al., 2016, 2018b) muscles.

**Pyruvate dehydrogenase E1 component subunit alpha, somatic form, mitochondrial.** Pyruvate dehydrogenase complex catalyzes the oxidative decarboxylation of pyruvate and its subsequent conversion to acetyl-CoA, $CO_2$, and NADH (Fregeau et al., 1990; Behal et al., 1993). Pyruvate dehydrogenase E1 was more abundant in LL3 mitochondria than in LL6 mitochondria. The E1 component (pyruvate dehydrogenase E1) is responsible for linking glycolysis to the TCA

cycle as the acetyl-CoA generated enters TCA cycle (Wang et al., 2016). Pyruvate content was greater in LL than PM during retail display (Abraham et al., 2017). Pyruvate dehydrogenase E1 is involved in the generation of NADH, which is required for metmyoglobin reduction in postmortem skeletal muscles (Bekhit and Faustman, 2005; Ramanathan et al., 2020a, 2020b). The greater abundance of pyruvate dehydrogenase E1 in LL3 steaks could replenish the pool of NADH that reduces metmyoglobin and thus contribute to the greater color stability of LL3 steaks compared with LL6 steaks.

**NADH dehydrogenase (ubiquinone) flavoprotein 1, mitochondrial.** NADH dehydrogenase (ubiquinone) flavoprotein 1 (NDUFV1) is a core subunit of the NADH dehydrogenase (complex 1), which is located in the inner mitochondrial membrane and is responsible for transferring the electrons from NADH to the respiratory chain. NDUFV1 was more abundant in mitochondria isolated from LL3 steaks compared with mitochondria from LL6 steaks. Belskie et al. (2015) reported that beef mitochondria could generate NADH via reverse electron flow, which can be used for metmyoglobin reduction through both electron transport–mediated and enzymatic pathways. The greater abundance of NDUFV1 in LL3 steaks may have resulted in greater production of NADH, which enhanced metmyoglobin reduction and improved color stability in LL3 steaks. In agreement, Yu et al. (2017a) documented that the subunits of NADH dehydrogenase exhibited positive correlations with redness of beef *semitendinosus* muscle.

**2-oxoglutarate dehydrogenase, mitochondrial.** The 2-oxoglutarate dehydrogenase complex (OGDHC) is primarily located within the mitochondria matrix and plays a key role in the TCA cycle (Qi et al., 2011). OGDHC was more abundant in mitochondria from LL3 steaks than in mitochondria from LL6 steaks. OGDHC mediates the decarboxylation of alpha-ketoglutarate; it catalyzes the conversion of 2-oxoglutarate to succinyl-CoA and $CO_2$ and generates NADH (Qi et al., 2011; Zhai et al., 2018). In postmortem skeletal muscles, NADH regeneration is closely associated with both enzymatic and nonenzymatic metmyoglobin reduction (Saleh and Watts, 1968; Renerre and Labas, 1987; Echevarne et al., 1990; Mancini and Hunt, 2005; Kim et al., 2006). The higher content of NADH confers a greater inherent ability to reduce metmyoglobin and, in turn, improves meat color stability (Ramanathan et al., 2020a, 2020b). The greater color stability in LL3 steaks could be due to the increased abundance of OGDHC, which increases the capacity to generate NADH for metmyoglobin reduction (Ramanathan et al., 2019).

**Mitochondrial aconitase 2.** Mitochondrial aconitase 2 (ACO2; also known as aconitate hydratase, mitochondrial) is an essential enzyme located in mitochondria. ACO2 is responsible for catalyzing the isomerization of citrate to isocitrate via cis-aconitate in the TCA cycle (Dickman and Speyer, 1954). ACO2 was identified in 4 spots, which were overabundant in LL3 mitochondria compared with LL6 mitochondria. These spots demonstrated different isoelectric points but similar molecular weight (Figure 3), which indicated possible posttranslational modifications (Gianazza, 1995; Halligan et al., 2004; Lengqvist et al., 2011; Zhang et al., 2020). The greater content of ACO2 in LL3 compared with in LL6 might indicate an increased rate of the conversion of citrate to isocitrate in the TCA cycle, which generates NADH that can be utilized for metmyoglobin reduction (Ramanathan et al., 2020a, 2020b). The resulting pool of NADH could have contributed to the greater color stability of LL3 steaks. On the other hand, previous studies (Joseph et al., 2012; Yu et al., 2017b) observed a greater abundance of ACO2 in sarcoplasm of color-labile beef PM compared with color-stable LL, possibly due to mitochondrial degeneration (Mitacek et al., 2018).

**Transferrin.** Transferrin, an iron binding transport protein synthesized in liver (Sayd et al., 2006), is responsible for delivering iron to the cells (Bekhit et al., 2013). Transferrin contains 2 iron binding sites on a single peptide chain (Decker and Mei, 1996). Transferrin was identified in 2 spots, and both of these spots were overabundant in mitochondria isolated from LL3 steaks compared with LL6 steaks. The 2 transferrin spots demonstrated different isoelectric points but similar molecular weight (Figure 3). The variation in isoelectric pH could be attributed to posttranslational modifications (Gianazza, 1995; Halligan et al., 2004; Lengqvist et al., 2011). In postmortem muscles, transferrin plays a protective role by binding free iron and thus inhibiting lipid oxidation (Decker and Mei, 1996). Therefore, the overabundance of transferrin in LL3 can potentially minimize lipid oxidation, which in turn would increase color stability. In contrast, Joseph et al. (2012) documented that transferrin was more abundant in the sarcoplasmic proteome of color-labile beef PM compared with color-stable LL. Nair et al. (2018a) observed a lower abundance of transferrin in beef *semitendinosus*, which has moderate color stability compared with color-labile PM and

color-stable LL. Nevertheless, the exact mechanism by which this protein influences meat color is not clearly understood.

## Conclusions

PM steaks exhibited a rapid decline of both color stability and MRA compared with LL steaks. Proteome profiling indicated differential abundance of several mitochondrial proteins (enzymes, binding proteins, and metabolic proteins) between beef muscles and display days. The observed variations in beef color stability between muscles (LL vs. PM) and retail display duration (LL3 vs. LL6) may be partially attributed to the differences in mitochondrial proteome components. While previous studies have reported differences in mitochondrial functionality between beef LL and PM, the results of the present study suggest other biochemical mechanisms behind those differences and their relationship with color stability.

### *Acknowledgments*

This project was supported by the Agriculture and Food Research Initiative Grant 2012-67018-30156 from the USDA National Institute of Food and Agriculture.

## Literature Cited

Abraham, A., J. W. Dillwith, G. G. Mafi, D. L. VanOverbeke, and R. Ramanathan. 2017. Metabolite profile differences between beef longissimus and psoas muscles during display. Meat Muscle Biol. 1:18–27. https://doi.org/10.22175/mmb2016.12.0007.

AMSA. 2012. Meat color measurement guidelines. 2nd edition. American Meat Science Association, Champaign, IL.

Behal, R. H., D. B. Buxton, J. G. Robertson, and M. S. Olson. 1993. Regulation of the pyruvate dehydrogenase multienzyme complex. Annu. Rev. Nutr. 13:497–520. https://doi.org/10.1146/annurev.nu.13.070193.002433.

Bekhit, A. E. D., and C. Faustman. 2005. Metmyoglobin reducing activity. Meat Sci. 71:407–439. https://doi.org/10.1016/j.meatsci.2005.04.032.

Bekhit, A. E. D. A., D. L. Hopkins, F. T. Fahri, and E. N. Ponnampalam. 2013. Oxidative processes in muscle systems and fresh meat: Sources, markers, and remedies. Compr. Rev. Food Sci. F. 12:565–597. https://doi.org/10.1111/1541-4337.12027.

Belskie, K. M., C. B. Van Buiten, R. Ramanathan, and R. A. Mancini. 2015. Reverse electron transport effects on NADH formation and metmyoglobin reduction. Meat Sci. 105:89–92. https://doi.org/10.1016/j.meatsci.2015.02.012.

Bianchini, E., S. Testoni, A. Gentile, T. Cali, D. Ottolini, A. Villa, M. Brini, R. Betto, F. Mascarello, P. Nissen, D. Sandona, and R. Sacchetto. 2014. Inhibition of ubiquitin proteasome system rescues the defective sarco (endo) plasmic reticulum Ca2+-ATPase (SERCA1) protein causing Chianina cattle pseudomyotonia. J. Biol. Chem. 289:33073–33082. https://doi.org/10.1074/jbc.M114.576157.

Canto, A. C. V. C. S., B. R. C. Costa-Lima, S. P. Suman, M. L. G. Monteiro, F. M. Viana, A. P. A. A. Salim, M. N. Nair, T. J. P. Silva, and C. A. Conte-Junior. 2016. Color attributes and oxidative stability of longissimus lumborum and psoas major muscles from Nellore bulls. Meat Sci. 121:19–26. https://doi.org/10.1016/j.meatsci.2016.05.015.

Canto, A. C. V. C. S., S. P. Suman, M. N. Nair, S. Li, G. Rentfrow, C. M. Beach, T. J. P. Silva, T. L. Wheeler, S. D. Shackelford, A. Grayson, R. O. McKeith, and D. A. King. 2015. Differential abundance of sarcoplasmic proteome explains animal effect on beef Longissimus lumborum color stability. Meat Sci. 102:90–98. https://doi.org/10.1016/j.meatsci.2014.11.011.

Chai, J., Q. Xiong, P. P. Zhang, Y. Y. Shang, R. Zheng, J. Peng, and S. W. Jiang. 2010. Evidence for a new allele at the SERCA1 locus affecting pork meat quality in part through the imbalance of $Ca^{2+}$ homeostasis. Mol. Biol. Rep. 37:613–619. https://doi.org/10.1007/s11033-009-9872-0.

Christianson, D. W., and C. A. Fierke. 1996. Carbonic anhydrase: Evolution of the zinc binding site by nature and by design. Accounts Chem. Res. 29:331–339.

CIE. 1976. Official recommendations on uniform colour space, colour difference equations and metric colour terms. Publication no. 15 (E-1.3.1), suppl. 2. Commission Internationale de l'Eclairage, Paris, France.

Csordas, G., C. Renken, P. Varnai, L. Walter, D. Weaver, K. F. Buttle, T. Balla, C. A. Mannella, and G. Hajnoczky. 2006. Structural and functional features and significance of the physical linkage between ER and mitochondria. J. Cell Biol. 174:915–921. https://doi.org/10.1083/jcb.200604016.

Csordas, G., P. Varnai, T. Golenar, S. Roy, G. Purkins, T. G. Schneider, T. Balla, and G. Hajnoczky. 2010. Imaging interorganelle contacts and local calcium dynamics at the ER-mitochondrial interface. Mol. Cell. 39:121–132. https://doi.org/10.1016/j.molcel.2010.06.029.

Decker, E. A., and L. Mei. 1996. Antioxidant mechanisms and applications in muscle foods. 49th Annual Proceedings of the Reciprocal Meat Conference, Am. Meat Sci. Assoc., Chicago, IL. pp. 64–72.

Dickman, S. R., and J. F. Speyer. 1954. Factors affecting the activity of mitochondrial and soluble aconitase. J. Biol. Chem. 206:67–75.

Echevarne, C., M. Renerre, and R. Labas. 1990. Metmyoglobin reductase activity in bovine muscles. Meat Sci. 27:161–172. https://doi.org/10.1016/0309-1740(90)90063-C.

Eisner, V., G. Csordas, and G. Hajnoczky. 2013. Interactions between sarco-endoplasmic reticulum and mitochondria in cardiac and skeletal muscle–pivotal roles in $Ca^{2+}$ and reactive oxygen species signaling. J. Cell Biol. 126:2965–2978. https://doi.org/10.1242/jcs.093609.

Faustman, C., and R. G. Cassens. 1990. The biochemical basis for discoloration in fresh meat: A review. J. Muscle Foods.

1:217–243. https://doi.org/10.1111/j.1745-4573.1990.tb00366.x.

Faustman, C., Q. Sun, R. Mancini, and S. P. Suman. 2010. Myoglobin and lipid oxidation interactions: Mechanistic bases and control. Meat Sci. 86:86–94. https://doi.org/10.1016/j.meatsci.2010.04.025.

Fleischer, S., and M. Inui. 1989. Biochemistry and biophysics of excitation-contraction coupling. Annu. Rev. Biophys. Bio. 18:333–364. https://doi.org/10.1146/annurev.bb.18.060189.002001.

Fregeau, D. R., T. E. Roche, P. A. Davis, R. Coppel, and M. E. Gershwin. 1990. Primary biliary cirrhosis. Inhibition of pyruvate dehydrogenase complex activity by autoantibodies specific for E1 alpha, a non-lipoic acid containing mitochondrial enzyme. J. Immunol. 144:1671–1676.

Gagaoua, M., J. Hughes, E. C. Terlouw, R. D. Warner, P. P. Purslow, J. M. Lorenzo, and B. Picard. 2020. Proteomic biomarkers of beef colour. Trends Food Sci. Tech. 101:234–252. https://doi.org/10.1016/j.tifs.2020.05.005.

Gianazza, E. 1995. Isoelectric focusing as a tool for the investigation of post-translational processing and chemical modifications of proteins. J. Chromatogr. A. 705:67–87. https://doi.org/10.1016/0021-9673(94)01251-9.

Grubbs, J. K., A. N. Fritchen, E. Huff-Lonergan, J. C. Dekkers, N. K. Gabler, and S. M. Lonergan. 2013. Divergent genetic selection for residual feed intake impacts mitochondria reactive oxygen species production in pigs. J. Anim. Sci. 91:2133–2140. https://doi.org/10.2527/jas.2012-5894.

Gueugneau, M., C. Coudy Gandilhon, O. Gourbeyre, C. Chambon, L. Combaret, C. Polge, D., D. Taillandier, D. Attaix, B. Friguet, A. B. Maier, G. Butler-Browne, and D. Bechet. 2014. Proteomics of muscle chronological ageing in post-menopausal women. BMC Genomics. 15:1165. https://doi.org/10.1186/1471-2164-15-1165.

Guo, B., W. Zhang, R. K. Tume, N. J. Hudson, F. Huang, Y. Yin, and G. Zhou. 2016. Disorder of endoplasmic reticulum calcium channel components is associated with the increased apoptotic potential in pale, soft, exudative pork. Meat Sci. 115:34–40. https://doi.org/10.1016/j.meatsci.2016.01.003.

Hajnoczky, G., L. D. Robb-Gaspers, M. B. Seitz, and A. P. Thomas. 1995. Decoding of cytosolic calcium oscillations in the mitochondria. Cell. 82:415–424. https://doi.org/10.1016/0092-8674(95)90430-1.

Halligan, B. D., V. Ruotti, W. Jin, S. Laffoon, S. N. Twigger, and E. A. Dratz. 2004. ProMoST (Protein Modification Screening Tool): A web-based tool for mapping protein modifications on two-dimensional gels. Nucleic Acids Res. 32:W638–W644. https://doi.org/10.1093/nar/gkh356.

Hamelin, M., T. Sayd, C. Chambon, J. Bouix, B. Bibe, D. Milenkovic, H. Leveziel, M. Georges, A. Clop, P. Marinova, and E. Laville. 2007. Differential expression of sarcoplasmic proteins in four heterogeneous ovine skeletal muscles. Proteomics. 7:271–280. https://doi.org/10.1002/pmic.200600309.

Henriques, B. J., R. K. Olsen, P. Bross, and C. M. Gomes. 2010. Emerging roles for riboflavin in functional rescue of mitochondrial β-oxidation flavoenzymes. Curr. Med. Chem. 17:3842–3854. https://doi.org/10.2174/092986710793205462.

Hunt, M. C., and H. B. Hedrick. 1977. Profile of fiber types and related properties of five bovine muscles. J. Food Sci. 42:513–517. https://doi.org/10.1111/j.1365-2621.1977.tb01535.x.

Izquierdo, J. M. 2006. Control of the ATP synthase β subunit expression by RNA-binding proteins TIA-1, TIAR, and HuR. Biochem. Bioph. Res. Co. 348:703–711. https://doi.org/10.1016/j.bbrc.2006.07.114.

Johnson, J. D., J. G. Mehus, K. Tews, B. I. Milavetz, and D. O. Lambeth. 1998. Genetic evidence for the expression of ATP- and GTP-specific succinyl-CoA synthetases in multicellular eucaryotes. J. Biol. Chem. 273:27580–27586. https://doi.org/10.1074/jbc.273.42.27580.

Joseph, P., S. P. Suman, G. Rentfrow, S. Li, and C. M. Beach. 2012. Proteomics of muscle-specific beef color stability. J. Agr. Food Chem. 60:3196–3203. https://doi.org/10.1021/jf204188v.

Ke, Y., R. M. Mitacek, A. Abraham, G. G. Mafi, D. L. VanOverbeke, U. Desilva, and R. Ramanathan. 2017. Effects of muscle-specific oxidative stress on cytochrome c release and oxidation-reduction potential properties. J. Agr. Food Chem. 65:7749–7755. https://doi.org/10.1021/acs.jafc.7b01735.

Kim, Y. H., M. C. Hunt, R. A. Mancini, M. Seyfert, T. M. Loughin, D. H. Kropf, and J. S. Smith. 2006. Mechanism for lactate-color stabilization in injection-enhanced beef. J. Agr. Food Chem. 54:7856–7862. https://doi.org/10.1021/jf061225h.

Kim, Y. H., J. T. Keeton, S. B. Smith, L. R. Berghman, and J. W. Savell. 2009. Role of lactate dehydrogenase in metmyoglobin reduction and color stability of different bovine muscles. Meat Sci. 83:376–382. https://doi.org/10.1016/j.meatsci.2009.06.009.

Kirchofer, K. S., C. B. Calkins, and B. L. Gwartney. 2002. Fiber–type composition of muscles of the beef chuck and round. J. Anim. Sci. 80:2872–2878. https://doi.org/10.2527/2002.80112872x.

Lanari, M. C., and R. G. Cassens. 1991. Mitochondrial activity and beef muscle color stability. J. Food Sci. 56:1476–1479. https://doi.org/10.1111/j.1365-2621.1991.tb08619.x.

Lawler, J. M., W. S. Barnes, G. Wu, W. Song, and S. Demaree. 2002. Direct antioxidant properties of creatine. Biochem. Bioph. Res. Co. 290:47–52. https://doi.org/10.1006/bbrc.2001.6164.

Ledward, D. A. 1985. Post-slaughter influences on the formation of metmyoglobin in beef muscles. Meat Sci. 15:149–171. https://doi.org/10.1016/0309-1740(85)90034-8.

Lengqvist, J., H. Eriksson, M. Gry, K. Uhlen, C. Bjorklund, B. Bjellqvist, P. J. Jakobsson, and J. Lehtio. 2011. Observed peptide pI and retention time shifts as a result of post-translational modifications in multidimensional separations using narrow-range IPG-IEF. Amino Acids. 40:697–711. https://doi.org/10.1007/s00726-010-0704-2.

Lindskog, S. 1997. Structure and mechanism of carbonic anhydrase. Pharmacol. Therapeut. 74:1–20. https://doi.org/10.1016/S0163-7258(96)00198-2.

Lohman, D. C., F. Forouhar, E. T. Beebe, M. S. Stefely, C. E. Minogue, A. Ulbrich, J. A. Stefely, S. Sukumar, M. Luna-Sanchez, A. Jochem, and S. Lew. 2014. Mitochondrial COQ9 is a lipid-binding protein that associates with COQ7 to enable coenzyme Q biosynthesis. P. Natl. Acad. Sci. USA. 111:E4697–E4705. https://doi.org/10.1073/pnas.1413128111.

Madhavi, D. L., and C. E. Carpenter. 1993. Aging and processing affect color, metmyoglobin reductase and oxygen consumption of beef muscles. J. Food Sci. 58:939–942. https://doi.org/10.1111/j.1365-2621.1993.tb06083.x.

Maia Research Analysis. 2020. Global Meat Wastage at Store or Losses Due to Discoloration of Meat 2015–2020. Maia Research Analysis report purchased July 20, 2020.

Mancini, R. A., and M. C. Hunt. 2005. Current research in meat color. Meat Sci. 71:100–121. https://doi.org/10.1016/j.meatsci.2005.03.003.

Mancini, R. A., K. Belskie., S. P. Suman, and R. Ramanathan. 2018. Muscle-specific mitochondrial functionality and its influence on fresh beef color stability. J. Food Sci. 83:2077–2082. https://doi.org/10.1111/1750-3841.14219.

Mancini, R. A., S. P. Suman, M. K. R. Konda, and R. Ramanathan. 2009. Effect of carbon monoxide packaging and lactate-enhancement on the color stability of beef steaks stored at 1°C for 9 days. Meat Sci. 81:71–76. https://doi.org/10.1016/j.meatsci.2008.06.021.

Marino, R. M. Albenzio, A. Della Malva, M. Caroprese, A. Santillo, and A. Sevi. 2014. Changes in meat quality traits and sarcoplasmic proteins during aging in three different cattle breeds. Meat Sci. 98:178–186. https://doi.org/10.1016/j.meatsci.2014.05.024.

Masuda, T., Y. Wada, and S. Kawamura. 2016. ES1 is a mitochondrial enlarging factor contributing to form mega-mitochondria in zebrafish cones. Science Reports. 6:22360. https://doi.org/10.1038/srep22360.

McAndrew, R. P., Y. Wang, A. W. Mohsen, M. He, J. Vockley, and J. J. P. Kim. 2008. Structural basis for substrate fatty acyl chain specificity crystal structure of human very-long-chain acyl-CoA dehydrogenase. J. Biol. Chem. 283:9435–9443. https://doi.org/10.1074/jbc.M709135200.

McKenna, D. R., P. D. Mies, B. E. Baird, K. D. Pfeiffer, J. W. Ellebracht, and J. W. Savell. 2005. Biochemical and physical factors affecting discoloration characteristics of 19 bovine muscles. Meat Sci. 70:665–682. https://doi.org/10.1016/j.meatsci.2005.02.016.

McLeish, M. J., and G. L. Kenyon. 2005. Relating structure to mechanism in creatine kinase. Crit. Rev. Biochem. Mol. 40:1–20. https://doi.org/10.1080/10409230590918577.

Mitacek, R. M., Y. Ke, J. E. Prenni, R. Jadeja, D. L. VanOverbeke, G. G. Mafi, and R. Ramanathan. 2018. Mitochondrial degeneration, depletion of NADH, and oxidative stress decrease color stability of wet-aged beef longissimus steaks. J. Food Sci. 84:38–50. https://doi.org/10.1111/1750-3841.14396.

Mohan, A., M. C. Hunt, S. Muthukrishnan, T. J. Barstow, and T. A. Houser. 2010. Myoglobin redox form stabilization by compartmentalized lactate and malate dehydrogenases. J. Agr. Food Chem. 58:7021–7029. https://doi.org/10.1021/jf100714g.

Møller, J. V., C. Olesen, A. M. L. Winther, and P. Nissen. 2010. The sarcoplasmic $Ca^{2+}$-ATPase: Design of a perfect chemi-osmotic pump. Q. Rev. Biophys. 43:501–566. https://doi.org/10.1017/S003358351000017X.

Nair, M. N., S. Li, C. M. Beach, G. Rentfrow, and S. P. Suman. 2018a. Changes in the sarcoplasmic proteome of beef muscles with differential color stability during postmortem aging. Meat Muscle Biol. 2:1–17. https://doi.org/10.22175/mmb2017.07.0037.

Nair, M. N., S. Li, C. Beach, G. Rentfrow, and S. P. Suman. 2018b. Intramuscular variations in color and sarcoplasmic proteome of beef semimembranosus during postmortem aging. Meat Muscle Biol. 2:92–101. https://doi.org/10.22175/mmb2017.11.0055.

Nair, M. N., S. P. Suman, M. K. Chatli, S. Li, P. Joseph, C. M. Beach, and G. Rentfrow. 2016. Proteome basis for intramuscular variation in color stability of beef semimembranosus. Meat Sci. 113:9–16. https://doi.org/10.1016/j.meatsci.2015.11.003.

Neethling, N. E., S. P. Suman, G. O. Sigge, L. C. Hoffman, and M. C. Hunt. 2017. Exogenous and endogenous factors influencing color of fresh meat from ungulates. Meat Muscle Biol. 1:253–275. https://doi.org/10.22175/mmb2017.06.0032.

Nierobisz, L. S. 2010. Molecular mechanisms characterizing skeletal muscle phenotype and function. Ph.D. dissertation, North Carolina State University, Raleigh, NC.

O'Keeffe, M., and D. E. Hood. 1982. Biochemical factors influencing metmyoglobin formation on beef from muscles of differing colour stability. Meat Sci. 7:209–228. https://doi.org/10.1016/0309-1740(82)90087-0.

Ostergaard, E. 2008. Disorders caused by deficiency of succinate-CoA ligase. J. Inherit. Metab. Dis. 31:226–229. https://doi.org/10.1007/s10545-008-0828-7.

Qi, F., R. K. Pradhan, R. K. Dash, and D. A. Beard. 2011. Detailed kinetics and regulation of mammalian 2-oxoglutarate dehydrogenase. BMC Biochem. 12:53. https://doi.org/10.1186/1471-2091-12-53.

Ramanathan, R., and R. A. Mancini. 2010. Effects of pyruvate on bovine heart mitochondria-mediated metmyoglobin reduction. Meat Sci. 86:738–741. https://doi.org/10.1016/j.meatsci.2010.06.014.

Ramanathan, R., and R. A. Mancini. 2018. Role of mitochondria in beef color: A review. Meat Muscle Biol. 2:309–320. https://doi.org/10.22175/mmb2018.05.0013.

Ramanathan, R., M. C. Hunt, R. A. Mancini, M. N. Nair, M. L. Denzer, S. P. Suman, and G. G. Mafi. 2020a. Recent updates in meat color research: Integrating traditional and high-throughput approaches. Meat Muscle Biol. 4:7, 1–24. https://doi.org/10.22175/mmb.9598.

Ramanathan, R., R. M. Mitacek, S. D. Billups, R. Jadeja, M. M. Pfeiffer, G. G. Mafi, and D. L. VanOverbeke, 2018. Novel nitrite-embedded packaging improves surface redness of dark-cutting longissimus steaks. Translational Animal Science. 2:135–143. https://doi.org/10.1093/tas/txy006.

Ramanathan, R., M. N. Nair, M. C. Hunt, and S. P. Suman. 2019. Mitochondrial functionality and beef colour: A review of recent research. S. Afr. J. Anim. Sci. 49:9–19. https://doi.org/10.4314/sajas.v49i1.2.

Ramanathan, R., S. P. Suman, and C. Faustman. 2020b. Biomolecular interactions governing fresh meat color in postmortem skeletal muscle: A review. J. Agr. Food Chem. 68:12779–12787. https://doi.org/10.1021/acs.jafc.9b08098.

Renerre, M., and R. Labas. 1987. Biochemical factors influencing metmyoglobin formation in beef muscles. Meat Sci. 19:151–165. https://doi.org/10.1016/0309-1740(87)90020-9.

Rossi, A. E., S. Boncompagni, and R. T. Dirksen. 2009. Sarcoplasmic reticulum-mitochondrial symbiosis: Bidirectional signaling in skeletal muscle. Exerc. Sport Sci. Rev. 37:29–35. https://doi.org/10.1097/JES.0b013e3181911fa4.

Saleh, B., and B. M. Watts. 1968. Substrates and intermediates in the enzymatic reduction of metmyoglobin in ground beef. J. Food Sci. 33:353–358. https://doi.org/10.1111/j.1365-2621.1968.tb03629.x.

Sammel, L. M., M. C. Hunt, D. H. Kropf, K. A. Hachmeister, and D. E. Johnson. 2002. Comparison of assays for metmyoglobin reducing ability in beef inside and outside semimembranosus muscle. J. Food Sci. 67:978–984. https://doi.org/10.1111/j.1365-2621.2002.tb09439.x.

Sayd, T., M. Morzel, C. Chambon, M. Franck, P. Figwer, C. Larzul, P. Le Roy, G. Monin, P. Cherel, and E. Laville. 2006. Proteome analysis of the sarcoplasmic fraction of pig semimembranosus muscle: Implications on meat color development. J. Agr. Food Chem. 54:2732–2737. https://doi.org/10.1021/jf052569v.

Schilling, M. W., S. P. Suman, X. Zhang, M. N. Nair, M. A. Desai, K. Cai, M. A. Ciaramella, and P. J. Allen. 2017. Proteomic approach to characterize biochemistry of meat quality defects. Meat Sci. 132:131–138. https://doi.org/10.1016/j.meatsci.2017.04.018.

Schlater, A. E., D. Miranda Jr., M. A. Frye, S. J. Trumble, and S. B. Kanatous. 2014. Changing the paradigm for myoglobin: A novel link between lipids and myoglobin. J. Appl. Physiol. 117:307–315. https://doi.org/10.1152/japplphysiol.00973.2013.

Sestili, P., C. Martinelli, G. Bravi, G. Piccoli, R. Curci, M. Battistelli, E. Falcieri, D. Agostini, A. M. Gioacchini, and V. Stocchi. 2006. Creatine supplementation affords cytoprotection in oxidatively injured cultured mammalian cells via direct antioxidant activity. Free Radical Bio. Med. 40:837–849. https://doi.org/10.1016/j.freeradbiomed.2005.10.035.

Sestili, P., C. Martinelli, E. Colombo, E. Barbieri, L. Potenza, S. Sartini, and C. Fimognari. 2011. Creatine as an antioxidant. Amino Acids. 40:1385–1396. https://doi.org/10.1007/s00726-011-0875-5.

Seyfert, M., R. A. Mancini, M. C. Hunt, J. Tang, C. Faustman, and M. Garcia. 2006. Color stability, reducing activity, and cytochrome c oxidase activity of five bovine muscles. J. Agr. Food Chem. 54:8919–8925. https://doi.org/10.1021/jf061657s.

Shen, L. Y., J. Luo, H. G. Lei, Y. Z. Jiang, L. Bai, M. Z. Li, G. Q. Tang, X. W. Li, S. H. Zhang, and L. Zhu. 2015. Effects of muscle fiber type on glycolytic potential and meat quality traits in different Tibetan pig muscles and their association with glycolysis-related gene expression. Genet. Mol. Res. 14:14366–14378. https://doi.org/10.4238/2015. November.13.22.

Silverman, D. N., and S. Lindskog. 1988. The catalytic mechanism of carbonic anhydrase: Implications of a rate-limiting protolysis of water. Accounts Chem. Res. 21:30–36. https://doi.org/10.1021/ar00145a005.

St-Pierre, J., J. A. Buckingham, S. J. Roebuck, and M. D. Brand. 2002. Topology of superoxide production from different sites in the mitochondrial electron transport chain. J. Biol. Chem. 277:44784–44790. https://doi.org/10.1074/jbc.M207217200.

Suman, S. P., and P. Joseph. 2013. Myoglobin chemistry and meat color. Annu. Rev. Food Sci. T. 4:79–99. https://doi.org/10.1146/annurev-food-030212-182623.

Suman, S. P., M. C. Hunt, M. N. Nair, and G. Rentfrow. 2014. Improving beef color stability: Practical strategies and underlying mechanisms. Meat Sci. 98:490–504. https://doi.org/10.1016/j.meatsci.2014.06.032.

Szabadkai, G., K. Bianchi, P. Varnai, D. De Stefani, M. R. Wieckowski, D. Cavagna, A. I. Nagy, T. Balla, and R. Rizzuto. 2006. Chaperone-mediated coupling of endoplasmic reticulum and mitochondrial $Ca^{2+}$ channels. J. Cell Biol. 175:901–911. https://doi.org/10.1083/jcb.200608073.

Szklarczyk, D., A. Franceschini, S. Wyder, K. Forslund, D. Heller, J. Huerta-Cepas, M. Simonovic, A. Roth, A. Santos, K. P. Tsafou. 2015. STRING v10: Protein–protein interaction networks, integrated over the tree of life. Nucleic Acids Res. 43:D447–D452. https://doi.org/10.1093/nar/gku1003.

Tang, J., C. Faustman, T. A. Hoagland, R. A. Mancini, M. Seyfert, and M. C. Hunt. 2005. Postmortem oxygen consumption by mitochondria and its effects on myoglobin form and stability. J. Agr. Food Chem. 53:1223–1230. https://doi.org/10.1021/jf048646o.

Toyoshima, C., and G. Inesi. 2004. Structural basis of ion pumping by $Ca^{2+}$-ATPase of the sarcoplasmic reticulum. Annu. Rev. Biochem. 73:269–292. https://doi.org/10.1146/annurev.biochem.73.011303.073700.

Utsumi, S., K. Sakamoto, T. Yamashita, H. Tomita, E. Sugano, K. Ishida, E. Ishiyama, and T. Ozaki. 2020. Presence of ES1 homolog in the mitochondrial intermembrane space of porcine retinal cells. Biochem. Bioph. Res. Co. 524:542–548. https://doi.org/10.1016/j.bbrc.2020.01.127.

Vasilaki, A., D. Simpson, F. McArdle, L. McLean, R. J. Beynon, H. Van Remmen, A. G. Richardson, A. McArdle, J. A. Faulkner, and M. J. Jackson. 2007. Formation of 3-nitrotyrosines in carbonic anhydrase III is a sensitive marker of oxidative stress in skeletal muscle. Proteom. Clin. Appl. 1:362–372. https://doi.org/10.1002/prca.200600702.

Von Seggern, D. D., C. R. Calkins, D. D. Johnson, J. E. Brickler, and B. L. Gwartney. 2005. Muscle profiling: Characterizing the muscles of the beef chuck and round. Meat Sci. 71:39–51. https://doi.org/10.1016/j.meatsci.2005.04.010.

Wallimann, T., M. Wyss, D. Brdiczka, K. Nicolay, and H. M. Eppenberger. 1992. Intracellular compartmentation, structure and function of creatine kinase isoenzymes in tissues with high and fluctuating energy demands: the 'phosphocreatine circuit' for cellular energy homeostasis. Biochem. J. 281:21–40. https://doi.org/10.1042/bj2810021.

Wang, Y., and S. Hekimi. 2016. Understanding ubiquinone. Trends Cell Biol. 26:367–378. https://doi.org/10.1016/j.tcb.2015.12.007.

Wang, Z., F. He, W. Rao, N. Ni, Q. Shen, and D. Zhang. 2016. Proteomic analysis of goat Longissimus dorsi muscles with different drip loss values related to meat quality traits. Food Sci. Biotechnol. 25:425–431. https://doi.org/10.1007/s10068-016-0058-y.

Wu, S., X. Luo, X. Yang, D. L. Hopkins, Y. Mao, and Y. Zhang. 2020. Understanding the development of color and color stability of dark cutting beef based on mitochondrial proteomics. Meat Sci. 163:108046. https://doi.org/10.1016/j.meatsci.2020.108046.

Wu, W., Q. Q. Yu, Y. Fu, X. J. Tian, F. Jia, X. M. Li, and R. T. Dai. 2016. Towards muscle-specific meat color stability of Chinese

Luxi yellow cattle: A proteomic insight into post-mortem storage. J. Proteomics. 147:108–118. https://doi.org/10.1016/j.jprot.2015.10.027.

Xu, H., Y. Xu, X. Liang, Y. Wang, F. Jin, D. Liu, Y. Ma, H. Yuan, X. Song, and W. Zeng. 2013. Porcine skeletal muscle differentially expressed gene ATP5B: molecular characterization, expression patterns, and association analysis with meat quality traits. Mamm. Genome. 24:142–150. https://doi.org/10.1007/s00335-013-9446-2.

Yang, X., S. Wu, D. L. Hopkins, R. Liang, L. Zhu, Y. Zhang, and X. Luo. 2018. Proteomic analysis to investigate color changes of chilled beef longissimus steaks held under carbon monoxide and high oxygen packaging. Meat Sci. 142:23–31. https://doi.org/10.1016/j.meatsci.2018.04.001.

Yi, M., D. Weaver, and G. Hajnoczky. 2004. Control of mitochondrial motility and distribution by the calcium signal: A homeostatic circuit. J. Cell Biol. 167:661–672. https://doi.org/10.1083/jcb.200406038.

Yu, Q., W. Wu, X. Tian, M. Hou, R. Dai, and X. Li. 2017a. Unraveling proteome changes of Holstein beef M. semitendinosus and its relationship to meat discoloration during postmortem storage analyzed by label-free mass spectrometry. J. Proteomics. 154:85–93. https://doi.org/10.1016/j.jprot.2016.12.012.

Yu, Q., W. Wu, X. Tian, F. Jia, L. Xu, R. Dai, and X. Li. 2017b. Comparative proteomics to reveal muscle-specific beef color stability of Holstein cattle during post-mortem storage. Food Chem. 229:769–778. https://doi.org/10.1016/j.foodchem.2017.03.004.

Zhai, C., S. P. Suman, M. N. Nair, S. Li, X. Luo, C. M. Beach, B. N. Harsh, D. D. Boler, A. C. Dilger, and D. W. Shike. 2018. Supranutritional supplementation of vitamin E influences mitochondrial proteome profile of post-mortem longissimus lumborum from feedlot heifers. S. Afr. J. Anim. Sci. 48:1140–1147. https://doi.org/10.4314/sajas.v48i6.18.

Zhang, X., D. S. Antonelo, J. D. Hendrix, V. To, Y. L. Campbell, M. Von Staden, S. Li, S. P. Suman, W. Zhai, J. Chen, H. Zhu, and M. W. Schilling. 2020. Proteomic characterization of normal and woody breast meat from broilers of five genetic strains. Meat Muscle Biol. 4(1): 9, 1–17. https://doi.org/10.22175/mmb.8759.

Zhang, W., S. Xiao, E. J. Lee, and D. U. Ahn. 2011. Consumption of oxidized oil increases oxidative stress in broilers and affects the quality of breast meat. J. Agr. Food Chem. 59:969–974. https://doi.org/10.1021/jf102918z.